Modeling of Surface Roughness Effects on Glaze Ice Accretion

R. John Hansman Jr.* and Keiko Yamaguchi†
Massachusetts Institute of Technology, Cambridge, Massachusetts 02139
Brian Berkowitz‡
Sverdrup Technology, Inc., Middleburg Heights, Ohio 44130
and
Mark Potapczuk§
NASA Lewis Research Center, Cleveland, Ohio 44135

A series of experimental investigations focused on studying the cause and effect of surface roughness on accreting glaze ice surfaces were conducted. Detailed microvideo observations were made of glaze ice accretions on 1- to 4-in.-diam cylinders in three icing wind tunnels (the Data Products of New England 6-in. test facility, the NASA Lewis Icing Research Tunnel, and the B. F. Goodrich Ice Protection Research Facility). Infrared thermal video recordings were made of accreting ice surfaces in the Goodrich facility. Distinct zones of surface water behavior were observed: a smooth wet zone in the stagnation region with a uniform water film, a rough zone where surface tension effects caused coalescence of surface water into stationary beads, a horn zone where roughness elements grow into horn shapes, a runback zone where surface water ran back as rivulets, and a dry zone where rime feathers formed. The location of the transition from the smooth to the rough zone was found to migrate with time towards the stagnation point. The behavior of the transition appeared to be controlled by boundary-layer transition and bead formation mechanisms at the interface between the smooth and rough zones. Regions of wet ice growth and enhanced heat transfer were clearly visible in the infrared video recordings of glaze ice surfaces. A simple multizone modification to the current glaze ice accretion model was proposed to include spatial variability in surface roughness. A preliminary version of this model was implemented on the LEWICE ice accretion code and compared with experimental ice shapes. For one of the cases, running the multizone model significantly improved the prediction of the glaze ice shapes.

I. Introduction

CURRENT efforts to analytically model glaze ice accretion are hampered by insufficient knowledge of the accreting ice surface roughness. In glaze icing, which normally occurs at temperatures near freezing or high liquid water contents, there is insufficient convective heat transfer to remove all of the latent heat of freezing of the impinging supercooled water droplets. The local ice accretion rate is, therefore, controlled by the local convective heat transfer. The droplet impingement behavior also plays an important role in determining where on the surface this wet growth occurs and is the controlling factor in dry or rime ice growth where there is sufficient cooling to freeze the droplets on impact.

The local convective heat transfer from a surface is known to be strongly dependent on the ice surface roughness.[1] Because of the importance of the heat transfer behavior on the ice accretion rate, the surface roughness becomes an important factor in modeling glaze ice accretion. Current analytical models such as LEWICE[2] generally assume that the surface roughness is uniform and the effective sand grain roughness k is used as an input parameter in the code. In some cases ad hoc spatial heat transfer distributions have been used.[3] The magnitude of the roughness parameter k is normally determined empirically by comparison between predicted and experimental ice accretions.

The erratic performance of glaze ice accretion models and the empirical manner in which the surface roughness is treated indicate the need for a more deterministic treatment of the surface roughness. In the following, experimental investigations that focused on the roughness of accreting glaze surfaces will be presented as well as preliminary results of a simple modification to the LEWICE code, which attempts to treat the ice surface roughness in a more physical manner.

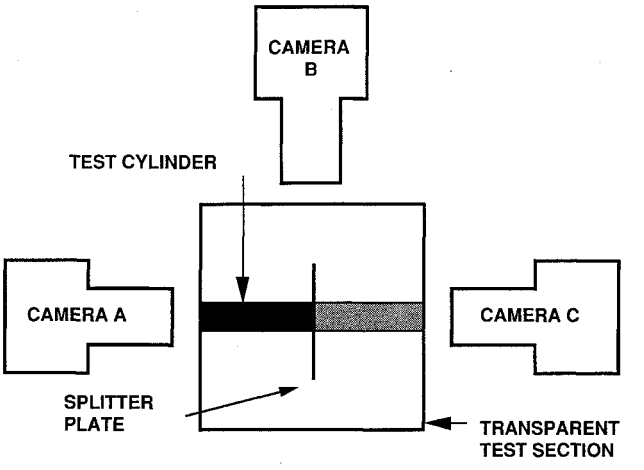

Fig. 1 Schematic view of the photographic set up for the DP and BFG icing tunnels.

Presented as Paper 89-0734 at the AIAA 27th Aerospace Sciences Meeting, Reno, NV, Jan. 9–12, 1989; received March 8, 1989; revision received Nov. 20, 1989.

*Associate Professor, Department of Aeronautics and Astronautics. Associate Fellow AIAA.
†Research Assistant, Department of Aeronautics and Astronautics. Student Member AIAA.
‡Engineering Associate.
§Aerospace Engineer. Member AIAA.

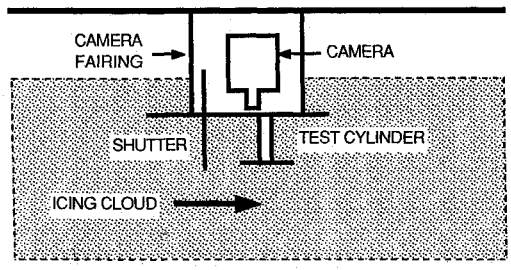

Fig. 2 Schematic view of the photographic setup in the IRT.

II. Experimental Setup for Ice Surface Observations

A. Experimental Facilities

Detailed observations of accreting ice surface roughness were made at several experimental icing facilities. These included the Data Products of New England small icing wind tunnel (6 in. × 6 in.), the NASA Icing Research Tunnel (9 ft × 7 ft), and the B. F. Goodrich Icing Wind Tunnel (2 ft × 4 ft). In the following, these facilities will be designated as DP, IRT, and BFG, respectively.

B. Photographic Setup

Detailed photographic observations of the behavior of surface water and formation of ice roughness on cylinders during glaze ice accretion were made in the three facilities described above. Cylinder diameters from 1 to 4 in. were observed. Freestream velocities of 100 and 150 kt were run at liquid water contents (LWC) up to 1.5 g/m^3. Tunnel total air temperatures varied from 0° to −10°C with some colder runs made for calibration purposes. In addition, a thremal infrared (IR) video system was used during the BFG tests to observe the relationship between surface temperature and surface roughness in glaze icing conditions.

The photographic setup used in the DP and BFG tests is shown in Fig. 1. The test articles were cylinders, which horizontally spanned the test section. The test-section walls were either Plexiglas (DP) or heated glass (BFG) to provide photographic access. Scale reference was provided by a grid mounted on a thin splitter plate at the midplane of the test section. A charge coupled device (CCD) microvideo (camera A) with a macrolens for magnification was used to obtain a grazing angle view of the ice accretion. The camera was focused at the stagnation region near the center of the test section. An additional video camera (camera B) was mounted slightly upstream of the cylinder to provide a view of the ice accretion looking normal to the cylinder surface. Secondary lighting was provided to obtain a clear video record of the accreting ice surface. A second grazing angle camera (camera C) was also used in some cases to provide a less magnified view of the overall ice shape.

The experimental setup used in the IRT tests is shown in Fig. 2. The photographic and test cylinder geometry is very similar to the DP and BFG grazing angle camera setup described previously. However, in order to locate the test cylinder within the region of uniform cloud, both the test cylinder and the camera had to be moved into the tunnel. A heated, waterproof fairing was provided to protect the camera. In addition, a shutter was located upstream to shield the test cylinder during initial transients in the liquid water content. Once the tunnel spray system had stabilized, the shield was removed and the cylinder began to ice. The nominal median volumetric diameter (MVD) used in the IRT tests was 20 μ.

C. Infrared Video Setup

The IR thermal video system setup used in the BFG tests is shown in Fig. 3. The IR camera was mounted above the test section. Because no IR transparent windows were available, a viewing slot was cut into the top of the tunnel so that the cylinder could be viewed directly. The IR video system provided color thermographs of the accreting ice surfaces and temperature profiles along designated sections. The system was typically operated with the color temperature scale set to 0.5°C and a dynamic range set between the tunnel operating temperature and 0°C. Cold air blowing out of the viewing slot cooled the IR optics and caused the absolute calibration of the system to drift. The system was, therefore, calibrated in situ by viewing points of known temperature while the tunnel was operating.

III. Experimental Observations of Ice Surface Roughness

A. Surface Roughness Zones

During the detailed photographic analyses of accreting ice surfaces, distinct regions were observed, each having a characteristic roughness and identifiable boundaries. A total of five roughness zones were identified, although rarely were more than three present on any particular ice accretion. The five zones are described briefly below.

1. Smooth Zone

In glaze ice accretions, close to the stagnation point, the surface was observed by light reflection and IR techniques to be uniformly wet with a thin film of water at warm temperatures. The surface in this regime was smooth, with no distinctly visible roughness. The ice was translucent within the smooth zone. The extent of the smooth zone can be seen in Fig. 4, which shows a representative final glaze ice shape for a 3-min icing exposure at 150 kt and −4.5°C at a liquid water content of 1.0 g/m^3 in the DP tunnel. Similar accretions were observed in IRT and BFG facilities.

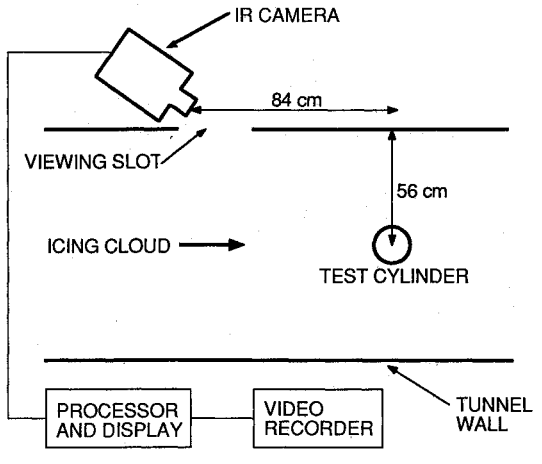

Fig. 3 Schematic view of the IR video system setup in the BFG icing tunnel.

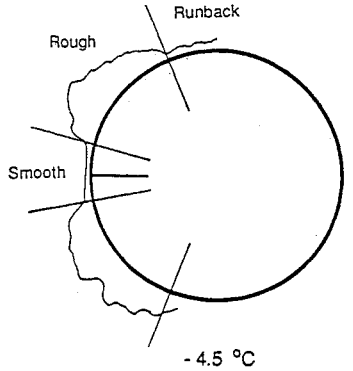

Fig. 4 Typical final glaze shape showing distinct roughness zones ($T = -4.5$°C, LWC = 1 g/m^3).

2. Rough Zone

At some point downstream, there was a sudden transition to a significantly rougher surface. This can be seen in Fig. 4. Within this zone, there appeared to be insufficient water to maintain a uniform film. Surface tension forces dominated the water surface behavior. Runback did not occur, rather, the water tended to coalesce into the water beads first observed by Olsen et al.[4,5] The scale length of the roughness was typically on the order of 1 mm.

Inasmuch as there was a distinct boundary between the smooth and rough zones, this position could be easily identified on the grazing angle video recording. The angular position of this boundary is plotted as a function of the time in Fig. 5 for the accretion shown in Fig. 4. The transition is observed to propagate rapidly towards the stagnation region. This behavior was observed in all three test facilities (DP, IRT, BFG). The repeatable nature of the smooth-rough transition's propagation towards the stagnation region implies a clear underlying physical mechanism for the transition between the surface water behavior in the smooth and rough zones. This is discussed in more detail in Sec. IIIB.

The ice accretion rate was observed to be enhanced in the rough zone as compared with the smooth zone. This can be seen in the ice profile shown in Fig. 4. The enhanced accretion rate is thought to be due to increased heat transfer resulting from the greater surface roughness in this zone. In all of the cases observed in this study, the ice horns characteristic of glaze ice accretion were found within the rough zone.

3. Horn Zone

In certain glaze ice accretions, particularly at high liquid water contents, some of the roughness elements within all or part of the rough zone were observed to grow into distinct protuberances. An example of such a case is shown in Fig. 6 for a very warm (−0.5°C) glaze ice accretion. Once these elements extended far enough above the ambient surface, they became essentially separate macroscopic ice accretions with high collection efficiencies catching droplets that would otherwise have been swept by the accreting body. Because of the collection efficiency and the enhanced heat transfer of these protuberances, they tended to grow rapidly resulting in horned ice accretions. In some warm cases, such as the one shown in Fig. 6, water was observed to be torn or shed from the individual elements. This results in a water-flow mechanism, which is not considered in any present ice accretion models.

4. Runback Zone

At warm temperatures a runback zone was observed aft of the rough zone in the primary accretion. An example can be seen in Fig. 4. This region was characterized by areas of ice interspersed with uniced surfaces. This ice was observed to form during an initial transition period after cloud exposure. The ice was translucent, and quite often frozen rivulets could be discerned. In warm conditions and high liquid water contents, the surface water was observed to initially runback and then stagnate at the point of flow separation. This water then slowly froze as rivulets or as large coalesced water cells. Once ice began to form in the upstream rough zone, no additional surface water was supplied to the runback zone, and the ice surface remained constant.

5. Rime Feather Zone

At cold temperatures rime feathers were sometimes observed to grow in the region aft of the primary accretion. The feathers were observed by the IR video system to be dry ice accretions and to propagate in the local upstream direction. It should be noted that there are intermediate conditions where neither runback or rime feathers are observed.

B. Effect of Icing Cloud Parameters on a Rough to Smooth Transition

The effect of icing cloud parameters on the transition between the smooth and rough surface zones was observed in an attempt to identify the underlying physical mechanisms which cause the rough surface to develop. The transition between the smooth and rough surface zones was monitored as a function of time for a variety of cloud conditions in the DP tunnel. The temperature, liquid water content, and freestream velocity effects were studied individually by holding all other parameters constant at nominal values and comparing transition behavior. The nominal velocity was 150 kt, the nominal liquid water content was approximately 0.4 g/m^3 with a MVD of 30 μ, and the nominal temperature was −4.5°C.

The effect of cloud temperature, liquid water content, and freestream velocity on the angular position of transition are shown as a function of time in Figs. 5, 7, and 8, respectively. In each case the transition point is observed to migrate toward the stagnation point as discussed previously. How-

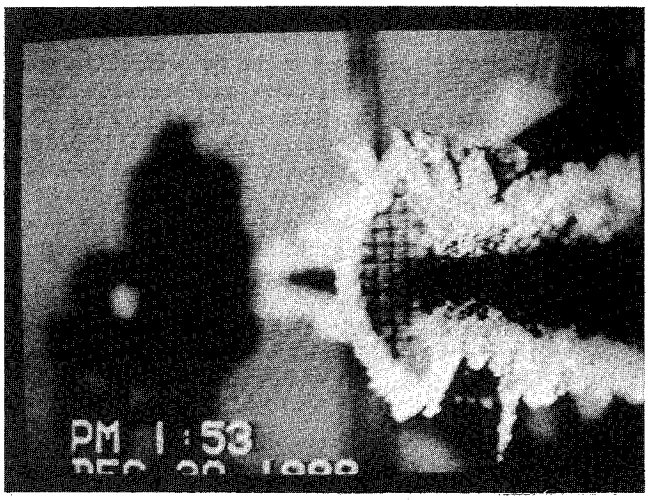

Fig. 6 Extreme example of horn elements for a warm glaze ice accretion (−0.5°C).

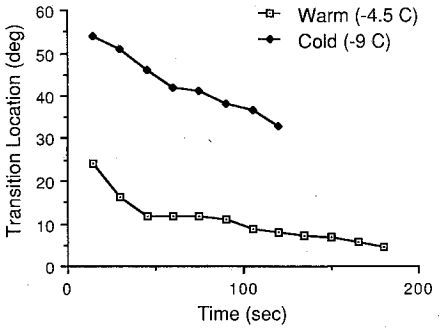

Fig. 5 Angular position vs time of smooth-rough transition location for two air temperatures.

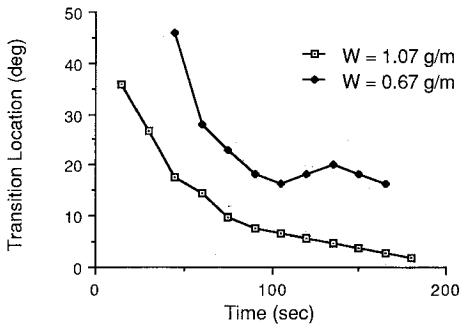

Fig. 7 Angular position vs time of smooth-rough transition location for two cloud liquid water contents.

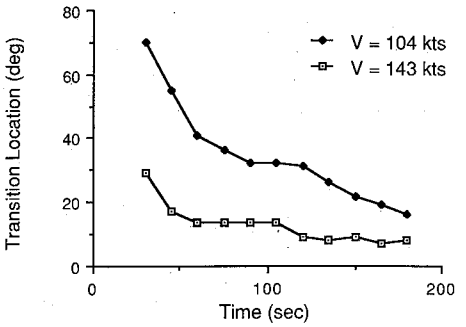

Fig. 8 Angular position vs time of smooth-rough transition for two freestream velocities.

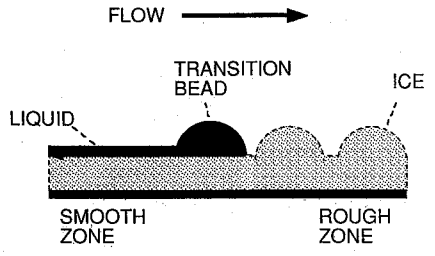

Fig. 9 Schematic representation of bead formation at the smooth to rough transition.

ever, a significant variation was observed in the actual transition location. It can be seen that warmer temperatures, increasing liquid water content, and increasing velocity tend to move the transition point closer to the stagnation region. These observations tend to imply that increasing Reynolds number and increasing the flow of surface water causes the smooth to rough transition point to move closer to the stagnation region.

The observed Reynolds number dependance may indicate that, in certain conditions, the initial transition in surface roughness is controlled by the boundary layer. In these cases the laminar to turbulent boundary-layer transition point will also be the initial smooth to rough transition point. The enhanced heat transfer in the turbulent region would cause sufficient freezing to partially dry the surface and cause bead formation, whereas in the laminar region the heat transfer is low enough that the surface is coated by a uniform water film. Once the roughness zone emerges, the roughness elements themselves will cause the transition of the boundary layer if it is not fully turbulated.

In order to more fully evaluate this hypothesis, the initial location of the rough to smooth transition was observed as a function of the Reynolds number for a variety of icing conditions in the IRT and BFG tunnels. The experimental data were compared with a simple boundary-layer transition model based on a critical roughness element Reynolds number. This comparison was complicated by the fact that the roughness element height in the stagnation region was observed to vary with freestream velocity. However, the experimental results appear consistent with the hypothesis that the initial rough to smooth transition is a result of the boundary-layer transition.

The influence of surface water flow on the rough to smooth transition location indicates that dynamic effects are also important. It is thought that the dynamic effects are caused by bead formation at the interface between the smooth and rough surface zones as is shown in Fig. 9. The formation of these beads at the interface causes enhanced heat transfer within the rough zone, which tends to freeze out the downstream beads and dry the surface. As the surface dries, beads begin to form further upstream and the transition point will propagate towards the stagnation region as observed experimentally. By increasing the surface water flux, the rate of formation and growth of the interfacial beads is increased. This causes the observed increase in upstream propagation of the transition point with surface water flux.

Further experimental observations are underway to more fully determine the boundary-layer and dynamic mechanisms which cause the transition in surface roughness.

C. Infrared Observations

Typical digitized video images of a 2.5-in. cylinder during a 2-min, 15-s icing encounter in the BFG tunnel are shown in Fig. 10. In this case the temperature was −4°C, the velocity was 150 kt, and the liquid water content was 1.5 gm/m^3. The IR camera was located 56 cm above and 84 cm upstream of the cylinder as shown in Fig. 3. As a result the cylinder was observed from above the horizontal, and only the top of the cylinder was in view. In the images, the flow would be from below, and a thermal profile corresponding to the midplane of the tunnel is shown on the right.

Prior to exposure to the icing cloud, in Fig. 10a, the cylinder was at a uniform temperature of −4°C corresponding to the tunnel stagnation temperature. When the spray was turned on, the stagnation region quickly warmed to 0°C indicating wet growth. The wet region spread for approximately 75 s until it reached equilibrium covering the forward 50 deg of the cylinder. The equilibrium wet region can be seen in Fig. 10b. As horned growth began to appear in the wet

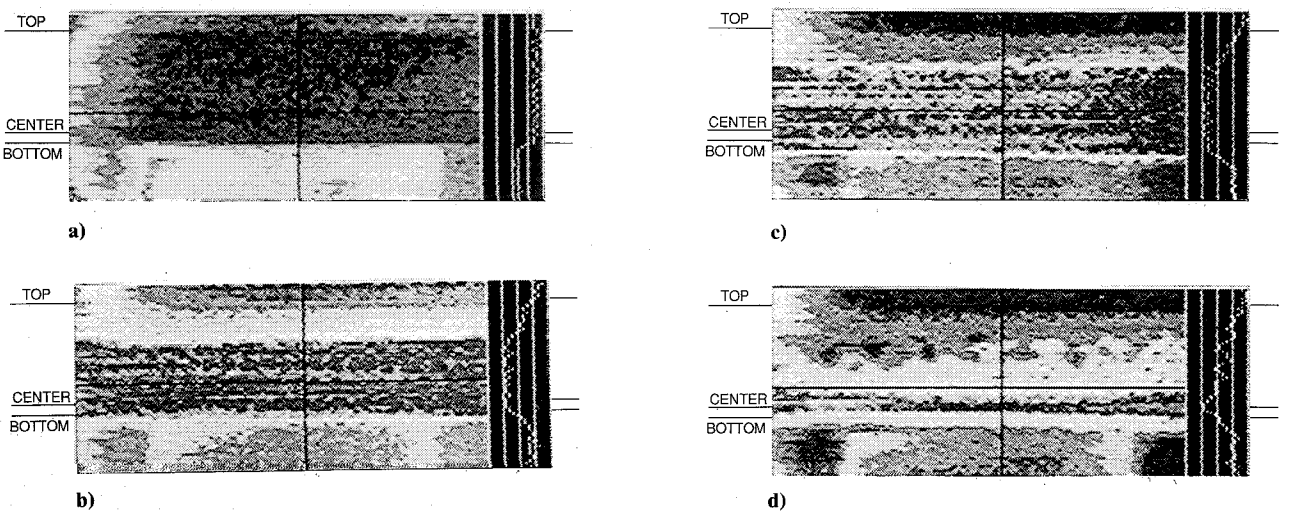

Fig. 10 Infrared thermographs of a 2.5-in. cylinder in the BFG tunnel (T = −4°C, V = 150 kt, LWC = 1.5 g/m^3): a) before icing cloud exposure, b) 75 s after exposure began, c) 135 s after exposure began, and d) 10 s after exposure ended.

region, the boundary of the wet region became irregular as exhibited in Fig. 10c. The enhanced heat transfer and the variation resulting from the rough surface and the horns can be seen in Fig. 10d, which was taken 10 s after the spray was shut off. At this time a small wet region can still be observed in the stagnation area due to the low heat transfer in that region.

The extent of the wet surface region was studied using the IR video system for a variety of conditions. It was found that both the surface roughness and horns were generated within the wet region. However, rime feathers were always observed in the dry region. The wet region was always centered around the stagnation line, and its extent varied as a function of icing conditions, particularly temperature. The angular extent of the wet region is plotted as a function of temperature in Fig. 11.

IV. Preliminary Implementation of a Multizone Model

A. Model Description

Based on the observations of surface water behavior during glaze accretion, a relatively simple modification to the existing ice accretion model is proposed, which may improve the current model's accuracy within the glaze ice regime. In this proposed "multizone" model, the accreting ice surface is divided into two or more discrete zones, which have varying surface water behavior and surface roughness. This is in contrast to current techniques, which assume that the surface has uniform roughness and surface water runback.

In the simplest version of the model, the surface is divided into two zones. There is a "smooth" wet zone corresponding to the smooth zone described in Sec. IIIA. It is centered about the stagnation region, and thin film runback occurs within the zone. In this region, the heat transfer would be that for a smooth surface and the Messinger[6]-type runback model used in existing codes such as LEWICE appears to be valid. No change in the existing codes is considered necessary in the smooth zone.

The remaining ice surface would consist of a "rough" zone where surface tension effects are important and characteristic water beads or roughness elements appear. Within this rough zone, the existing Messinger runback model is not appropriate for two reasons. First, the increased roughness will enhance the heat transfer and consequently increase the freezing fraction. Second, experimental observations by Olsen and Walker[4,5] and Hansman and Turnock[7,8] indicate that in some cases, surface water does not runback in the rough zone. In most cases surface tension forces dominate the water behavior, and the beads remain stationary on the surface. At warm temperatures, high liquid water contents, or high velocities, the beads may grow large enough that aerodynamic forces cause the beads to either slide aft on the surface or be torn from the surface and shed into the airflow.

In the absence of runback, the freezing fraction can be assumed to be unity within the rough region. This assumption obviates the need to calculate the convective heat transfer

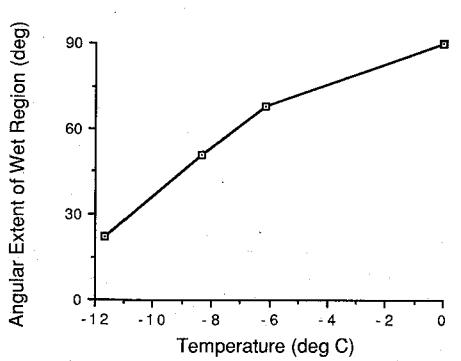

Fig. 11 Angular extent of wet region as a function of temperature for a 2.5-in. cylinders in the BFG tunnel (V = 150 kt, LWC = 1.0 g/m^3).

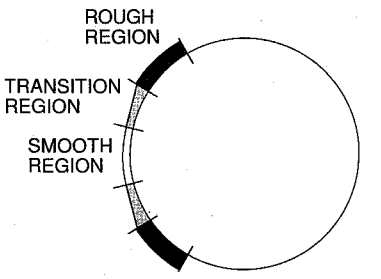

Fig. 12 Schematic representation of zones used in the model.

coefficient and the effective surface roughness, which greatly simplifies the ice accretion model. In the presence of runback or sliding, the freezing fraction is less than unity and must be computed by the model through the Messinger heat balance approach with appropriate heat transfer coefficients corresponding to the enhanced roughness. In some cases it may be adequate to approximate the spatial variation of the freezing fraction by linear interpolation between the smooth zone value and unity at the point where the rough zone ends or the surface is dry.

In the presence of shedding, the modeling is more complex. Some mechanism must be included to model the shedding process and the increased roughness within the rough zone. One approach would be to determine a maximum unfrozen water thickness for each element based on the local flow velocity. If the water layer in the element exceeds this value, the water is shed from the surface in the model to both the runback and heat transfer. The roughness within the rough zone could then be modeled as the maximum stable droplet size.

Because the boundary between the rough and smooth zones moves with time, it is necessary to incorporate this into the model. Since most ice accretion codes run a limited number of time steps, it was found to be convenient to include a third transition zone between the rough zones as shown in Fig. 12. For cases where there is no runback in the rough zone, the transition extends between the location of the rough to smooth transition at the beginning and end of the time step. For cases where there is runback in the rough zone, the transition region would extend between the rough to smooth transition and the end of the rough zone or the point at which there is no further runback. Under these assumptions, the freezing fraction can simply be ramped up in the transition zone from the smooth zone value to unity. It should be noted that, in principle, the surface roughness could be varied instead of the freezing fraction. This was attempted; however, difficulties were encountered in correlating the effective heat transfer and equivalent sand grain roughness used in LEWICE with physical values. Therefore, the freezing fraction approach was employed in these preliminary evaluations.

B. Results

A prototype of the proposed multizone model was implemented in the LEWICE code to evaluate the effectiveness of the concept. In this preliminary model, the rough to smooth transition location and the extent of the wet growth region were taken from experimental observations. The intermediate and final ice accretions profiles were compared with experimentally measured profiles for several cases.

One of the comparisons was conducted for a LWC of 0.35 g/m^3 on a 1-in. cylinder in the DP tunnel at -4.5°C and 150 kt. Since there was little or no runback in this case, the freezing fraction was ramped linearly through the transition zone from the smooth zone value to unity in the rough zone. The comparisons between the experimentally measured ice shapes and those predicted by the multizone LEWICE code and the normal LEWICE code with the Ruff roughness correlations[9] are shown in Fig. 13. It can be seen that there is a significant improvement in fidelity of the overall ice shape

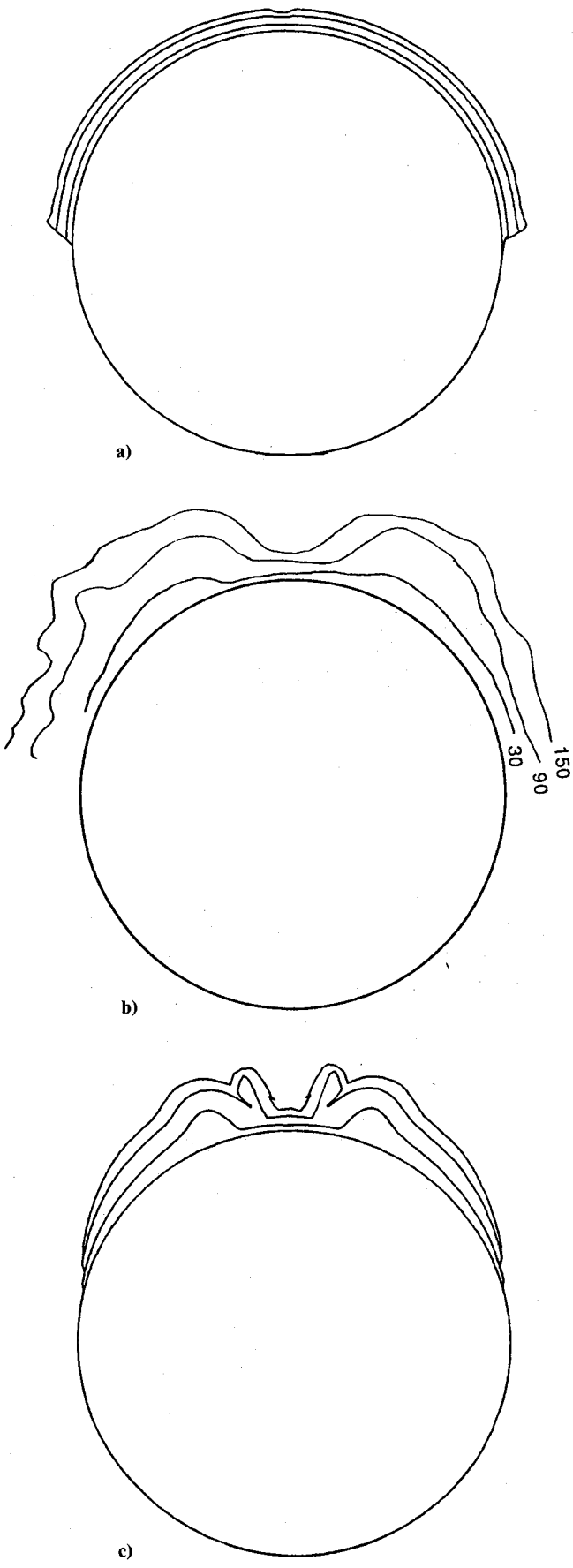

Fig. 13 Comparison of predicted and experimental ice shapes for a 1-in. cylinder ($T = -4.5°C$, $V = 150$ kt, LWC $= 0.35$ g/m^3): a) normal LEWICE at 45, 105, and 150 s; b) experimental result at 30, 90, and 150 s; and c) modified LEWICE at 45, 105, and 150 s.

for the multizone case. There is, however, an irregularity in the ice surface, which appears in the second time step and is thought to be an artifact of the ramped freezing fraction combined with the long time steps. The irregularity is located at the point where the freezing fraction becomes unity. Because of the relatively long time steps used in the simulation, runback water collects at this point resulting in the observed bulge. Efforts are underway to minimize this effect in a physically realistic and numerically acceptable manner. In general, however, the multizone LEWICE predicts the essential components of the ice accretion, whereas the normal LEWICE prediction is not at all representative of the experimentally observed ice shape.

V. Conclusions

The investigation into modeling of surface roughness effects on glaze accretion has resulted in the following.

1) Accreting glaze ice surfaces have been observed to have distinct zones of surface roughness. They include a smooth wet zone in the stagnation region where uniform runback occurs, a rough zone where surface tension causes coalescence of the surface water into beads, a horn zone which can emerge out of the rough zone with large roughness elements, a runback zone where surface water runs back as rivulets, and a zone where rime feathers grow.

2) The location of the transition point between the smooth and rough zone was observed to propagate with time towards the stagnation point.

3) The initial location of the surface roughness transition point appears to be related to the transition of the boundary layer from laminar to turbulent. The propagation of the transition point appears to be related to the rate of bead formation at the interface between the rough and smooth zones.

4) Infrared video observations were made of accreting ice surfaces. This technique was used to investigate the extent of wet regions on the ice surface and also measured heat transfer enhancements resulting from roughness and horn elements.

5) Based on the above, a preliminary modification to the LEWICE ice accretion code which incorporates multiple roughness zones was proposed.

6) The proposed multizone modifications were implemented using experimental data to determine factors such as the rough to smooth transition locations. The multizone modifications significantly improved the performance of the code as compared with the normal LEWICE code. Based on the good performance of the preliminary multizone code, further efforts to develop a more fully deterministic and optional version of the code appear to be warranted.

Acknowledgments

This work was supported in part by NASA and the Federal Aviation Administration under Grants NAG-3-666 and NGL-22-009-640. The work was also supported by the National Science Foundation Presidential Young Investigators Program, Award No. 8552702. Use of the icing wind-tunnel facilities were provided courtesy of Data Products of New England, B. F. Goodrich De-Icing Systems, and the NASA Lewis Research Center. Partial support for the infrared video equipment was provided by Hughes Aircraft Company. Dr. James Riley of the FAA Technical Center provided valuable input to the modeling efforts.

References

[1]Achenbach, E., "The Effect of Surface Roughness on the Heat Transfer from a Circular Cylinder to the Cross Flow of Air," *International Journal of Heat Mass Transfer*, Vol. 20, 1977, pp. 359–369.

[2]MacArthur, C. D., "Numerical Simulation of Airfoil Ice Accretion," AIAA Paper 83-0112, Jan. 1983.

[3]Gent, R. W., and Cansdale, J. T., "The Development of Mathematical Modeling Techniques for Helicopter Rotor Icing," AIAA Paper 85-0336, Jan. 1985.

[4]Olsen, W., and Walker, E., "Close up Motion Pictures of the Icing Process," NASA LeRC Film, 1983.

[5]Olsen, W., and Walker, E., "Experimental Evidence for Modifying the Current Physical Model for Ice Accretion on Aircraft Structures," NASA TM-87184, 1987.

[6]Messinger, B. L., "Equilibrium Temperature of an Unheated Icing Surface as a Function of Airspeed," *Journal of the Aeronautical Sciences*, Vol. 20, Jan. 1953, pp. 24–42.

[7]Hansman, R. J., and Turnock, S., "Investigation of Surface Water Behavior During Glaze Ice Accretion," AIAA Paper 88-0115, Jan. 1988.

[8]Hansman, R. J., and Turnock, S., "Investigation of Microphysical Factors Which Influence Surface Roughness During Glaze Ice Accretion," *Proceedings of the 4th International Workshop on the Atmospheric Icing of Structures*, Sept. 1988.

[9]LEWICE Users Manual, NASA CR-185129, NASA Lewis Research Center, Cleveland, OH, Sept. 1988.